Automatic Construction of control triangles for subdivided Powell-Sabin splines

Evelyne Vanraes, Joris Windmolders
Adhemar Bultheel, Paul Dierckx

Abstract

In this paper we present an algorithm for calculating the B–spline representation of a Powell–Sabin spline surface on a refinement of the given triangulation. The resulting subdivision scheme is a $\sqrt{3}$ scheme; a new vertex is added inside every original triangle. Applying the $\sqrt{3}$ scheme twice yields a triadic scheme, every original edge is split into three new edges, but special care is needed at the boundaries. The scheme is numerically stable and generally applicable, there are no restrictions on the initial triangulation.

Keywords: Powell–Sabin splines, subdivision, normalised B–splines, CAGD

AMS(MOS) classification: 65D07, 65D17, 68U07

1 Introduction

Geometric modelling of complex shapes relies heavily on the use of powerful mathematical representations of surfaces. Widely used now in CAGD packages is the tensor product B-spline representation, which is, however, restricted to rectangular domains, and therefore is not well suited for designing surfaces with an arbitrary number of edges. Farin's Bézier triangles [2] are a worthwhile alternative to represent piecewise polynomials on polygonal domains, but imposing smoothness conditions between the patches requires a great number of nontrivial relations between the coefficients to be satisfied. Another approach is a B-spline representation for Powell-Sabin (PS)-splines by Shi *et al.* [6], but their construction method has some serious drawbacks from the numerical point of view. Dierckx [1] presented an improved algorithm to construct a normalised B-spline basis for PS-splines, which guarantees global C^1 smoothness for any choice of the coefficients, and resolves the numerical problems. This representation also has a nice geometric interpretation involving tangent control triangles for manipulating the PS–surfaces.

For the graphical display of a surface we need a denser set of points that represent the surface, or in other words, we need a representation of the surface on a refinement of the triangulation on which it is defined. This procedure is called subdivision. Because after subdivision the new basis functions have smaller support, it also gives the designer more local control when manipulating surfaces. Windmolders and Dierckx [9] solved the subdivision problem for uniform Powell–Sabin splines, that is on triangulations with all equilateral triangles. In this paper we solve the subdivision problem for general Powell-Sabin splines.

Section 2 recalls some concepts of polynomials on triangulations and gives the definition of the space of Powell-Sabin splines. It also covers the relevant aspects of the construction of a normalised B-spline basis. In this work we are only interested in the functional case. Section 3 first gives an overview of possible subdivision schemes. Then the subdivision rules are developed for the case of $\sqrt{3}$ subdivision. The boundaries are treated separately to achieve a triadic scheme. Finally we conclude with some remarks and suggestions for further research in section 4.

2 Powell-Sabin splines

2.1 Polynomials on triangles

Let $\lambda = (\lambda_1, \lambda_2, \lambda_3)$, $|\lambda| = \lambda_1 + \lambda_2 + \lambda_3 = d$, $\lambda_i \in \{0, 1, \ldots, d\}$ using standard multi index notation. Consider a non degenerate triangle $\mathcal{T}(T_1, T_2, T_3)$ in a plane with its vertices having Cartesian coordinates $T_i(x_i, y_i), i = 1, 2, 3$. Any point $P(x, y)$ in that plane can be expressed in terms of barycentric coordinates $\tau = (\tau_1, \tau_2, \tau_3)$ with respect to $\mathcal{T}$: $P = \sum_{i=1}^{3} \tau_i T_i$ where $|\tau| = 1$.

A Bézier polynomial [2] of degree d over the triangle $\mathcal{T}$ is defined by

$$b^d_{\mathcal{T}}(P) = b^d_{\mathcal{T}}(\tau) = \sum_{|\lambda|=d} b_\lambda B^d_\lambda(\tau), \tag{2.1}$$

in which b_λ are called Bézier ordinates, and

$$B^d_\lambda(\tau) = \frac{d!}{\lambda_1!\lambda_2!\lambda_3!} \tau_1^{\lambda_1} \tau_2^{\lambda_2} \tau_3^{\lambda_3} \tag{2.2}$$

are the Bernstein-Bézier polynomials on the triangle.

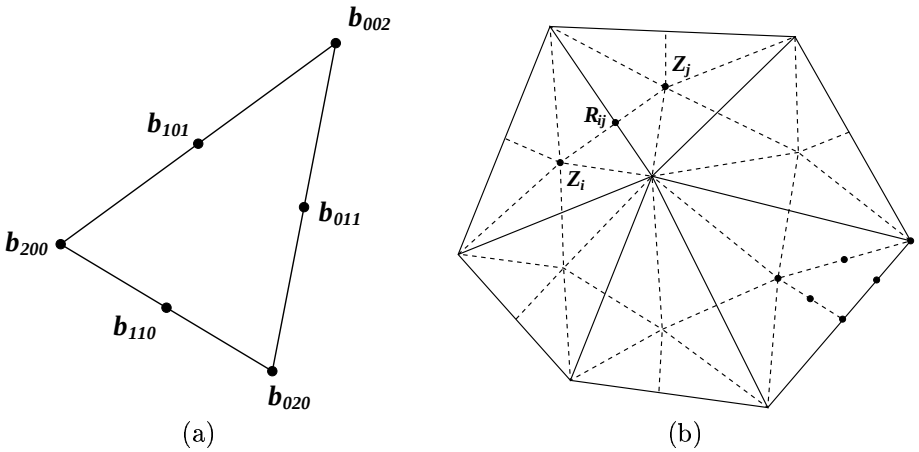

Figure 1. (a) Positions of Bézier ordinates for $d = 2$. (b) PS-refinement. Each triangle ρ_j is split into six smaller triangles with a common vertex Z_j.

The points $(\frac{\lambda}{d}, b_\lambda)$ are the control points for the surface $z = b^d_{\mathcal{T}}(\tau)$ and the piecewise linear interpolant to these points is the Bézier net or control net. This is displayed schematically in figure 1(a) for the case $d = 2$. The points $\frac{\lambda}{d}$, marked with dots on the figure, are called Bézier triangle points. The control net mimics the shape of the surface and is tangent to the polynomial surface at the three vertices of the triangle.

Representing complex shapes, however, requires the use of patch complexes with a great number of Bézier triangles. Keeping up continuity conditions between all the neighbouring patches then results, in general, in nontrivial relations between their Bézier ordinates. The use of split triangles can overcome this problem.

2.2 PS-splines

Consider a simply connected subset $\Omega \subset \mathbb{R}^2$ with polygonal boundary $\delta\Omega$. Suppose we have a conforming triangulation Δ of Ω, constituted of triangles ρ_j, $j = 1, \ldots, t$, having vertices V_k with Cartesian coordinates (x_k, y_k), $k = 1, \ldots, n$. Let Δ^* be a Powell-Sabin refinement of Δ, which divides each triangle ρ_j into six smaller triangles with a common vertex Z_j as follows (figure 1(b)) :

(1) Choose an interior point Z_j in each triangle ρ_j, so that if two triangles ρ_i and ρ_j have a common edge, then the line joining these interior points Z_i and Z_j intersects the common edge at a point R_{ij} between its vertices. Choosing Z_j as the incentre of each triangle ρ_j ensures the existence of the points R_{ij}. Other choices may be more appropriate from the practical point of view.

(2) Join each point Z_j to the vertices of ρ_j.

(3) For each edge of the triangle ρ_j
- which belongs to the boundary $\delta\Omega$, join Z_j to an arbitrary point of the edge.
- which is common to a triangle ρ_i, join Z_j to R_{ij}.

Now we consider the space of piecewise C^1 continuous quadratic polynomials on Δ^*, the Powell-Sabin splines. It is denoted by $S_2^1(\Delta^*)$. Each of the $6t$ triangles resulting from the PS-refinement becomes the domain triangle of a quadratic Bernstein-Bézier polynomial, i.e. we choose $d = 2$ in equation (2.1) and (2.2), as indicated for one subtriangle in figure 1(b). Powell and Sabin [5] proved that the dimension of the space $S_2^1(\Delta^*)$ equals $3n$: there exists a unique solution $s(x, y) \in S_2^1(\Delta^*)$ for the interpolation problem

$$s(V_k) = f_k, \quad \frac{\partial s}{\partial x}(V_k) = f_{x,k}, \quad \frac{\partial s}{\partial y}(V_k) = f_{y,k}, \quad k = 1, \ldots, n. \tag{2.3}$$

So given the function and derivative values at each vertex V_k, the Bézier ordinates on the domain subtriangles are uniquely defined and the continuity conditions between subtriangles are automatically fulfilled.

2.3 A normalised B-spline representation

Dierckx [1] showed that each piecewise polynomial $s(x, y) \in S_2^1(\Delta^*)$ has a unique representation

$$s(x, y) = \sum_{i=1}^{n} \sum_{j=1}^{3} c_{ij} B_i^j(x, y) \ , \quad (x, y) \in \Omega, \tag{2.4}$$

where the basis functions satisfy

$$B_i^j(x, y) \geq 0 \tag{2.5}$$

$$\sum_{i=1}^{n} \sum_{j=1}^{3} B_i^j(x, y) \equiv 1, \tag{2.6}$$

and have local support: $B_i^j(x, y)$ is nonzero only on the so-called 1-ring M_i of V_i, being the set of triangles ρ_l that have V_i as a vertex. The number of triangles in M_i is called the valence m_i.

To construct the basis functions $B_i^j(x, y)$ we use the algorithm from [1]. For each vertex this approach leads to a triangle $t_i(Q_{i1}, Q_{i2}, Q_{i3})$ with vertices $Q_{ij}(X_{ij}, Y_{ij})$ that must contain certain Bézier triangle points of the underlying Bézier representation. These Bézier triangle points shown as $S, \tilde{S}$, S' in figure 2 and we denote their barycentric coordinates with respect to t_i as (L_{i1}, L_{i2}, L_{i3}), $(\tilde{L}_{i1}, \tilde{L}_{i2}, \tilde{L}_{i3})$ and $(L_{i1}^{'}, L_{i3}^{'}, L_{i3}^{'})$. The triangles t_i, $i = 1, \ldots, n$ are called PS-triangles.

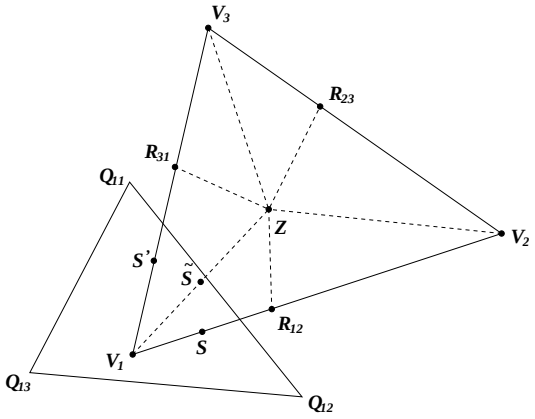

Figure 2: PS-points and PS-triangle.

We define the control points as

$$C_{ij} = (Q_{ij}, c_{ij}) = (X_{ij}, Y_{ij}, c_{ij}) \tag{2.7}$$

and the control triangles as

$$T_i(C_{i1}, C_{i2}, C_{i3}). \tag{2.8}$$

The projection of the control triangles T_i in the (x, y) plane are the PS-triangles t_i. One can prove that the control triangle T_i is tangent to the surface $z = s(x, y)$ at V_i. The tangent point is $(x_i, y_i, s(V_i))$. For design purposes we prefer the control points of the corresponding control triangle to be close to the surface. In [1] the PS-triangle with the smallest area is computed, but other choices are possible.

2.4 Bézier representation of a PS-spline

The Bézier representation of a PS-spline surface can be calculated from the B-spline representation. Consider a domain triangle $\rho(V_i, V_j, V_k) \in \Delta$ with its PS-refinement as on figure 3(a), where

$$\begin{aligned} R_{ij} &= \lambda_{ij} V_i + (1 - \lambda_{ij}) V_j \\ R_{jk} &= \lambda_{jk} V_j + (1 - \lambda_{jk}) V_k \\ R_{ki} &= \lambda_{ki} V_k + (1 - \lambda_{ki}) V_i \\ Z_{ijk} &= a_{ijk} V_i + b_{ijk} V_j + c_{ijk} V_k. \end{aligned} \tag{2.9}$$

Denote the Bézier ordinates as on figure 3(b). They can be written as the following unique convex barycentric combinations of the B-spline coefficients:

$$\begin{aligned} s_i &= \alpha_{i1} c_{i1} + \alpha_{i2} c_{i2} + \alpha_{i3} c_{i3} \\ u_i &= L_{i1} c_{i1} + L_{i2} c_{i2} + L_{i3} c_{i3} \\ v_i &= L'_{i1} c_{i1} + L'_{i2} c_{i2} + L'_{i3} c_{i3} \\ w_i &= \tilde{L}_{i1} c_{i1} + \tilde{L}_{i2} c_{i2} + \tilde{L}_{i3} c_{i3}. \end{aligned} \tag{2.10}$$

The coefficients in these formulae depend on the geometry of the PS-refinement, and on the choice of the PS-triangles. Similar expressions hold for (s_j, u_j, v_j, w_j) and (s_k, u_k, v_k, w_k). The other Bézier

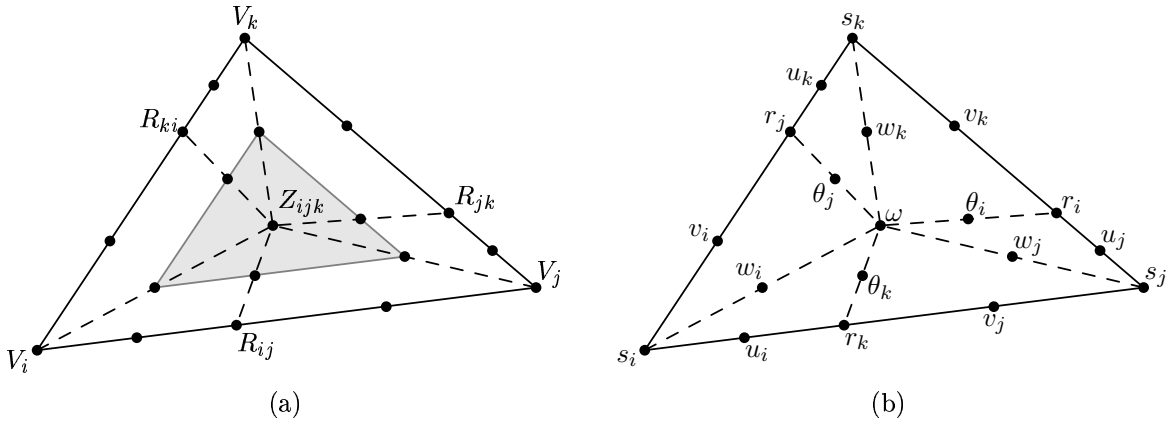

Figure 3. (a) PS-refinement of a triangle $\rho(V_i, V_j, V_k)$. (b) Schematic representation of Bézier ordinates.

ordinates can be found from the C^1 continuity conditions between the Bézier triangles, e.g.,

$$\begin{aligned} r_k &= \lambda_{ij} u_i + (1-\lambda_{ij}) v_j \\ \theta_k &= \lambda_{ij} w_i + (1-\lambda_{ij}) w_j \\ \omega &= a_{ijk} w_i + b_{ijk} w_j + c_{ijk} w_k. \end{aligned} \tag{2.11}$$

Consider the triangle $T_{ijk}^{\sqrt{3}}$ formed by the Bézier control points corresponding to the Bézier ordinates w_i, w_j and w_k. From the tangent property of the Bézier control net for each of the Bézier triangles in the PS-refinement follows that $T_{ijk}^{\sqrt{3}}$ is tangent to the surface at $(Z_{ijk}, w = s(Z_{ijk}))$. Notice that also the Bézier control points corresponding to θ_i, θ_j and θ_k lie in $T_{ijk}^{\sqrt{3}}$. The projection $t_{ijk}^{\sqrt{3}}$ of $T_{ijk}^{\sqrt{3}}$ in the (x,y)-plane is shaded in figure 3(a).

3 Subdivision

The goal of subdivision is to calculate the B-spline representation (2.4) of a PS-spline surface on a refinement Δ^1 of the given triangulation Δ^0. The new basis functions after subdivision have smaller support and give the designer more local control when manipulating surfaces. Adjusting one coefficient c_{ij} of a control point of a subdivided PS-spline surface, influences a smaller neighbourhood of the involved vertex. The control triangles are tangent to the surface and in case of repeated subdivision, the linear interpolant of the tangent points converges to the surface itself. Therefore subdivision is a common technique for displaying surfaces graphically.

In section 3.1 we consider different possibilities for the refinement Δ^1 of the original triangulation Δ^0. This answers the question where to place the new vertices. Then, in section 3.2, we derive the subdivision rules for the $\sqrt{3}$ scheme. It turns out that the triangle $T_{ijk}^{\sqrt{3}}$ can be used as the control triangle for a new vertex. The boundaries are treated separately.

3.1 Choosing a suitable refinement Δ^1 of Δ^0

3.1.1 *Dyadic subdivision*

The most obvious possibility is dyadic subdivision. In this scheme a new vertex is inserted on every edge between two old vertices and every original triangle is split into four new triangles.

When choosing the positions of the new vertices, the lines of the PS-refinement Δ^{0*} of the initial triangulation Δ^0 must be maintained in the PS-refinement Δ^{1*} of the refined triangulation Δ^1, because the aim is to represent exactly the same surface. To ensure this, the new vertices have to be placed on the intersections R_{ij} of the PS-refinement with the edges. For the new triangle (V_{ij}, V_{jk}, V_{ki}) the PS-refinement is already fixed, the point Z_{ijk} is the interior point for this triangle. The interior points for the three remaining triangles have to lie on the line of the old PS-refinement Δ^{0*} that crosses the new triangle. The refined triangulation is shown in figure 4.

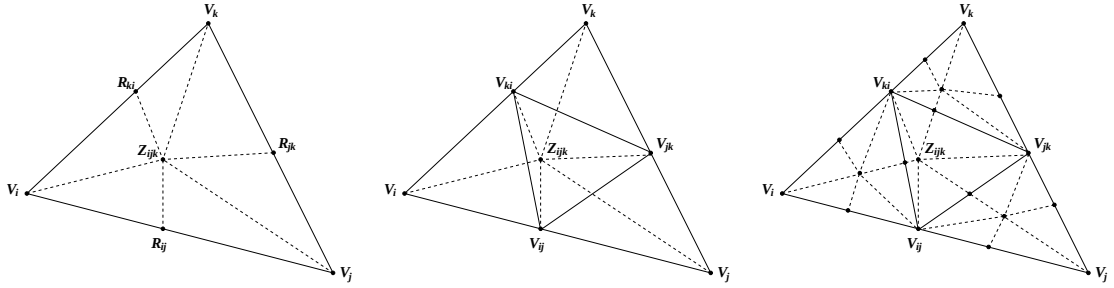

Figure 4. Positions of the new vertices and PS-refinement in the new triangles for dyadic subdivision.

The dyadic scheme was used by Windmolders and Dierckx for uniform Powell-Sabin splines, this is on a triangulation with all equilateral triangles. The subdivision rules for this special case can be found in [9]. In the general case the idea of dyadic subdivision can only be used under certain conditions. For example, the point Z_{ijk} of the PS-refinement of a triangle, must lie inside the middle triangle $(V_{ij}V_{jk}V_{ki})$. This leads to conditions on the initial triangulation Δ^0 and its PS-refinement Δ^{0*}, i.e. on the placement of the interior points Z_{ijk} and the resulting positions of the R_{ij}: the dyadic scheme is not generally applicable.

3.1.2 $\sqrt{3}$ *subdivision*

Another possiblity is $\sqrt{3}$ subdivision. This kind of scheme was first introduced by Kobbelt [3] and Labsik and Greiner [4] and used for uniform Powell-Sabin splines by Vanraes *et al.* [8]. The new triangulation $\Delta^{\sqrt{3}}$ is constructed by inserting a new vertex V_{ijk} at the position of the interior point Z_{ijk} of each triangle. Except at the boundaries, the old edges are not preserved in the new triangulation. Instead new edges are introduced connecting every new vertex V_{ijk} with the vertices of the old triangle it lies in, and connecting every two new vertices that lie in neighbouring old triangles. Figure 5(b) shows the result of $\sqrt{3}$ subdivision on the triangulation Δ^0 of figure 5(a). In this figure the PS-refinement is not shown, but note that the new edges in $\Delta^{\sqrt{3}}$ must coincide with the lines of the PS-refinement Δ^{0*} and that the original edges of Δ^0 are now part of the new PS-refinement $\Delta^{\sqrt{3}*}$.

Figure 6 shows a detail of one original triangle after $\sqrt{3}$ subdivision. In the new triangles new interior points must be chosen on the one line of the new PS-refinement $\Delta^{\sqrt{3}*}$ that is already fixed, that is, the original edge that crosses the triangle. For example

$$\begin{aligned} Z_{ij} &= \omega_{ij} V_i + (1 - \omega_{ij}) R_{ij}, \\ Z_{ji} &= \omega_{ji} V_j + (1 - \omega_{ji}) R_{ij}. \end{aligned} \tag{3.1}$$

For the resulting refinement to exist, the new vertex V_{ijk} has to lie inside the hexagon formed by

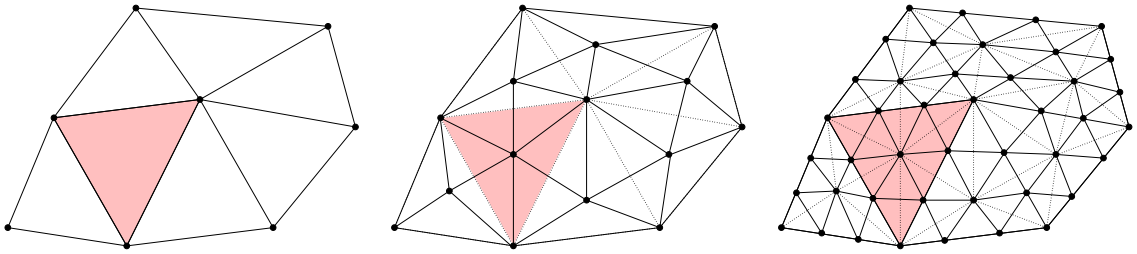

Figure 5. Principle of $\sqrt{3}$-subdivision. Applying $\sqrt{3}$-subdivision twice results in triadic subdivision. The PS-refinements are not shown.

the interior points $(Z_{ij}, Z_{ji}, Z_{jk}, Z_{kj}, Z_{ki}, Z_{ik})$. It is always possible to place these interior points, i.e. choose a value for ω in equation (3.1), such that this condition is fulfilled: there are no conditions on the initial triangulation Δ^0 or its PS-refinement Δ^{0*}. Therefore we prefer to use the $\sqrt{3}$ scheme instead of the dyadic scheme.

In a practical implementation we use $\omega = 1/3$ because this leads to the expected results in the uniform case when all triangles are equilateral and have the same size. We check whether the result satisfies the hexagon requirement and in the occasional case that is does not, we decrease the value incrementally, e.g. by dividing it by a factor 2, until it yields a valid PS-refinement.

Applying the $\sqrt{3}$ subdivision operator a second time, again results in new vertices that coincide with the interior points that in this case lie on the edges of the initial triangulation. As can be seen in figure 5(c), this causes a refinement trisecting of every original edge and splitting each original triangle into nine subtriangles. Hence one single refinement step of this scheme can be considered as the square root of one step of a triadic scheme.

In order to achieve a triadic scheme for splines defined on a bounded domain, the boundary triangles have to be treated different in the second $\sqrt{3}$ step. Instead of inserting one new vertex in the interior of the boundary triangle, we insert two new vertices on the boundary edge such that the result is the same as if there would have been a neighbouring triangle. For this reason we always do two $\sqrt{3}$ steps in a practical implementation.

3.2 Calculating the refined B-spline representation

3.2.1 *The triangles $t_{ijk}^{\sqrt{3}}$ and $T_{ijk}^{\sqrt{3}}$*

We now show that the triangles $T_{ijk}^{\sqrt{3}}$, introduced in the last paragraph of section 2.4, can act as control triangles for the new vertices V_{ijk}. Recall that such a triangle is defined by three particular Bézier control points as shown in figure 3(a). We denote these new control points by $C_{ijk,1}^{\sqrt{3}}$, $C_{ijk,2}^{\sqrt{3}}$ and $C_{ijk,3}^{\sqrt{3}}$. The corners of the corresponding PS-triangle $t_{ijk}^{\sqrt{3}}$ are then $Q_{ijk,1}^{\sqrt{3}}$, $Q_{ijk,2}^{\sqrt{3}}$ and $Q_{ijk,3}^{\sqrt{3}}$.

Theorem 3.1 *The triangle $T_{ijk}^{\sqrt{3}}$ is a valid control triangle for the new vertex V_{ijk}. The B-spline coefficients are*

$$\begin{aligned} C_{ijk,1}^{\sqrt{3}} &= \tilde{L}_{i1}C_{i1} + \tilde{L}_{i2}C_{i2} + \tilde{L}_{i3}C_{i3} \\ C_{ijk,2}^{\sqrt{3}} &= \tilde{L}_{j1}C_{j1} + \tilde{L}_{j2}C_{j2} + \tilde{L}_{j3}C_{j3} \\ C_{ijk,3}^{\sqrt{3}} &= \tilde{L}_{k1}C_{k1} + \tilde{L}_{k2}C_{k2} + \tilde{L}_{k3}C_{k3}. \end{aligned} \tag{3.2}$$

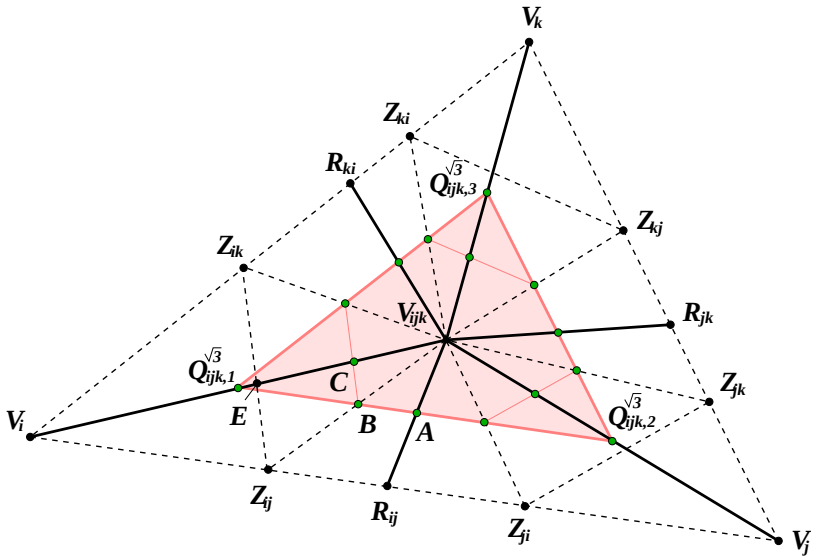

Figure 6. $\sqrt{3}$ subdivision: $t^{\sqrt{3}}_{ijk}$ is a valid PS-triangle for V_{ijk}. A valid choice for the new interior points and the PS-refinement always exist, there are no conditions on the initial triangulation.

Proof: To prove that $T^{\sqrt{3}}_{ijk}$ is indeed a valid control triangle, we first need to prove that $t^{\sqrt{3}}_{ijk}$ is a valid PS-triangle, or in other words, that $t^{\sqrt{3}}_{ijk}$ contains all the involved PS-points. The valence m_{ijk} of V_{ijk} is always six and there are twelve PS-points, shown as gray dots in figure 6, plus the vertex V_{ijk} itself, that have to be contained in the new PS-triangle. The proposed PS-triangle $t^{\sqrt{3}}_{ijk}$ is marked in gray. We can see that the corners $Q^{\sqrt{3}}_{ijk}$ of this triangle are PS-points of the original PS-refinement Δ^{0*} that lie in the middle between V_{ijk} and the old vertices. We now zoom in on the left bottom corner and check that the PS-points A, B and C of $\Delta^{\sqrt{3}*}$ are contained in the proposed PS-triangle $t^{\sqrt{3}}_{ijk}$.

Referring to (2.9) and (3.1) it immediately follows that

$$A = \lambda_{ij} Q^{\sqrt{3}}_{ijk,1} + (1-\lambda_{ij}) Q^{\sqrt{3}}_{ijk,2} \tag{3.3}$$

and

$$\begin{aligned} B &= \omega_{ij} Q^{\sqrt{3}}_{ijk,1} + (1-\omega_{ij}) A \\ &= (\omega_{ij} + \lambda_{ij} - \omega_{ij}\lambda_{ij}) Q^{\sqrt{3}}_{ijk,1} + (1 - \lambda_{ij} - \omega_{ij} + \omega_{ij}\lambda_{ij}) Q^{\sqrt{3}}_{ijk,2}. \end{aligned} \tag{3.4}$$

Denote by E the intersection of $Z_{ij}Z_{ik}$ and $V_{ijk}V_i$. We can determine $0 < r < 1$ such that

$$E = rV_i + (1-r)V_{ijk}, \tag{3.5}$$

$$\begin{aligned} C &= \frac{1}{2}(E + V_{ijk}) \\ &= rQ^{\sqrt{3}}_{ijk,1} + (1-r)V_{ijk}, \\ &= ((1-r)a_{ijk} + r) Q^{\sqrt{3}}_{ijk,1} + (1-r) b_{ijk} Q^{\sqrt{3}}_{ijk,2} + (1-r) c_{ijk} Q^{\sqrt{3}}_{ijk,3}. \end{aligned} \tag{3.6}$$

From (3.3), (3.4) and (3.6) we see that the barycentric coordinates of A, B and C with respect to $t_{ijk}^{\sqrt{3}}$ are all positive, which means that they lie inside or on the boundary of the triangle $t_{ijk}^{\sqrt{3}}$. This is independent of the value for ω_{ij} that was used in equation (3.1) to determine the position of the interior point Z_{ij}. The same reasoning can be used for the remaining PS-points of V_{ijk} and we conclude that $t_{ijk}^{\sqrt{3}}$ is a valid PS-triangle for the vertex V_{ijk} after one $\sqrt{3}$ subdivision step.

For the corresponding triangle $T_{ijk}^{\sqrt{3}}$ to be a valid control triangle, it needs to be tangent to the surface at V_{ijk}. This follows from the tangent property of the Bézier control net as already mentioned in section 2.4.

From Equation (2.10) we know that

$$\begin{aligned} c_{ijk,1}^{\sqrt{3}} &= \tilde{L}_{i1}c_{i1} + \tilde{L}_{i2}c_{i2} + \tilde{L}_{i3}c_{i3} \\ c_{ijk,2}^{\sqrt{3}} &= \tilde{L}_{j1}c_{j1} + \tilde{L}_{j2}c_{j2} + \tilde{L}_{j3}c_{j3} \\ c_{ijk,3}^{\sqrt{3}} &= \tilde{L}_{k1}c_{k1} + \tilde{L}_{k2}c_{k2} + \tilde{L}_{k3}c_{k3}. \end{aligned} \tag{3.7}$$

The same convex combinations also apply to $Q_{ijk}^{\sqrt{3}}$ and consequently also to $C_{ijk}^{\sqrt{3}}$.
□

□

The formulas (3.7) use only convex combinations of the old data. The barycentric coordinates $\tilde{L}$ have values between 0 and 1. This means that the subdivision scheme is numerically stable.

3.2.2 *Boundaries*

If the triangle (V_i, V_j, V_k) has no neighbouring triangle $(V_i, V_j, V_{k'})$, i.e. the edge V_iV_j is a boundary edge, we need different rules for the second $\sqrt{3}$ step to achieve a trisection of the edge V_iV_j. Instead of inserting one new vertex in the interior of the boundary triangle, we insert two new vertices on the boundary edge on the positions where they would have been if there was a neighbouring triangle.

For these vertices, V_{ij} and V_{ji} on figure 7 we propose a different PS-triangle that uses only information of the triangle (V_i, V_j, V_k). The control points $C_{ij,1}$ and $C_{ij,3}$ are calculated with the standard formulas. From the tangent property of the Bézier control net we know that $C_{ij,2}$ can be written as a linear combination of the two Bézier ordinates u_i and v_j from figure 3

$$\begin{aligned} C_{ij,2} &= \omega_{ij}u_i + (1-\omega_{ij})r_k \\ &= \omega_{ij}u_i + (1-\omega_{ij})(\lambda_{ij}u_i + (1-\lambda_{ij})v_j) \\ &= (\omega_{ij} + \lambda_{ij} - \omega_{ij}\lambda_{ij})u_i + (1-\omega_{ij} - \lambda_{ij} + \omega_{ij}\lambda_{ij})v_j \\ &= (\omega_{ij} + \lambda_{ij} - \omega_{ij}\lambda_{ij})(L_{i1}Q_{i1} + L_{i2}Q_{i2} + L_{i3}Q_{i3}) \\ &\quad + (1-\omega_{ij} - \lambda_{ij} + \omega_{ij}\lambda_{ij})(L_{j1}Q_{j1} + L_{j2}Q_{j2} + L_{j3}Q_{j3}). \end{aligned} \tag{3.8}$$

Note that because

$$\begin{aligned} \omega_{ij} + \lambda_{ij} - \omega_{ij}\lambda_{ij} &= \omega_{ij}(1-\lambda_{ij}) + \lambda_{ij} > 0 \\ &= 1 - (1-\omega_{ij})(1-\lambda_{ij}) < 1. \end{aligned} \tag{3.9}$$

this special rule is a convex combination of the data on the previous level: the algorithm is also numerically stable at the boundaries.

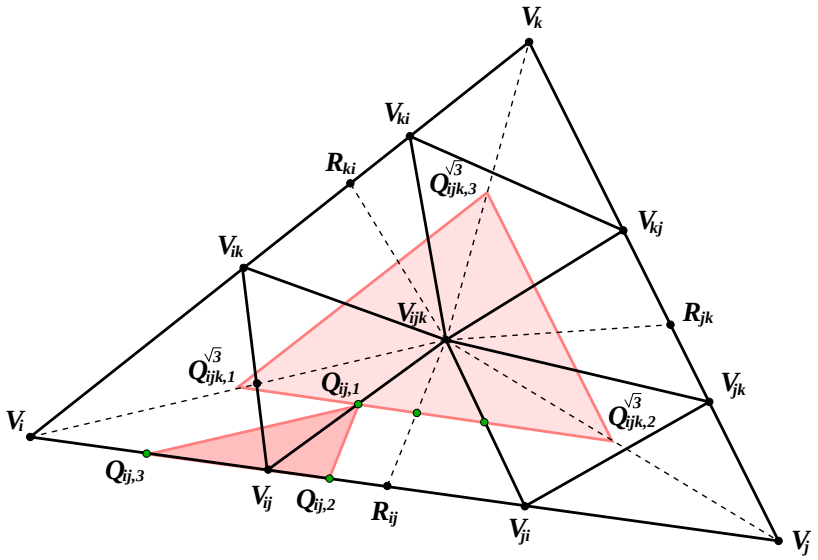

Figure 7. For vertices V_{ij} on a boundary edge we choose a different control triangle that only uses information of the triangle $(V_iV_jV_k)$.

3.2.3 *Further optimisation*

For the original vertices we can reuse their original control triangles. This is a valid choice because after subdivision, the PS-points are closer to the involved vertex and are therefore contained in the PS-triangle. It is however possible to choose a smaller PS-triangle, rescale t_i and denote the new PS-triangle with t_i'.

To find the appropriate scaling factor, we need to know the positions of the interior points of the PS-refinement $\Delta^{\sqrt{3}*}$. For example in the triangle $V_iV_{ijk}V_{ijk'}$ where V_{ijk} is the new vertex in the neighbouring triangle $(V_iV_jV_{k'})$ we choose the interior point Z_{ij} between R_{ij} and V_i

$$Z_{ij} = \omega_i V_i + (1-\omega_i)V_{ijk}, \qquad 0 < \omega_i < 1 \tag{3.10}$$

and we suggest to choose the same value ω_i for the interior points of all triangles that have V_i as a vertex. It is this value ω_i that we use to rescale t_i to t_i', i.e.

$$\begin{aligned} C'_{i1} &= (\omega_i\alpha_{i1} + 1 - \omega_i)\, C_{i1} + \omega_i\alpha_{i2}\, C_{i2} + \omega_i\alpha_{i3}\, C_{i3} \\ C'_{i2} &= \omega_i\alpha_{i1}\, C_{i1} + (\omega_i\alpha_{i2} + 1 - \omega_i)\, C_{i2} + \omega_i\alpha_{i3}\, C_{i3} \\ C'_{i3} &= \omega_i\alpha_{i1}\, C_{i1} + \omega_i\alpha_{i2}\, C_{i2} + (\omega_i\alpha_{i3} + 1 - \omega_i)\, C_{i3}. \end{aligned} \tag{3.11}$$

4 Concluding remarks

In this paper we have proposed an algorithm for computing the B-spline representation of a Powell-Sabin surface on a refinement of the given triangulation. We haven chosen a $\sqrt{3}$ subdivision scheme because there are no restrictions on the initial triangulation, as opposed to a dyadic scheme. Triadic subdivision can be seen as two subsequent steps of $\sqrt{3}$ subdivision. For new vertices on the boundaries of the initial triangulation special rules apply every second $\sqrt{3}$ step. Since the algorithm uses only convex combinations it is numerically stable.

For a triangulation with a certain PS-refinement, there are different possibilities for the control and PS-triangles. The only requirement is that a PS-triangle must contain all its PS-points. In [1] the control triangle with the smallest area is chosen, because then the control points are close to the surface. This leads to a quadratic programming problem. The control triangles of the new vertices are optimal in this sense. The scaling operation on the control triangles of the old vertices does not result in optimal triangles but the control triangle shrinks in each step. This is important because otherwise the basis functions become linearly dependent.

Wavelets can be developed with the technique of the lifting scheme with the subdivision scheme as the prediction step and an extra update step [7]. This was already done for uniform Powell-Sabin splines in [10], but was not yet possible in the general case.

Acknowledgement

This work is partially supported by the Belgian Program on Interuniversity Poles of Attraction, initiated by the Belgian State, Prime Minister's Office for Science, Technology and Culture, and by the Flemish Fund for Scientific Research (FWO VLaanderen) project MISS (G.0211.02). The scientific responsibility rests with the authors.

Bibliography

1. P. Dierckx. On calculating normalized Powell–Sabin B–splines. *CAGD*, 15(1):61–78, 1997.
2. G. Farin. Triangular Bernstein–Bézier patches. *CAGD*, 3(2):83–128, 1986.
3. Leif Kobbelt. $\sqrt{3}$–subdivision. In *Computer Graphics Proceedings*, Annual Conference Series. ACM SIGGRAPH, 2000.
4. U. Labsik and G. Greiner. Interpolatory $\sqrt{3}$-subdivision. In Sabine Coquillart and Jr. Duke, David, editors, *Proceedings of the 21th European Conference on Computer Graphics (Eurographics-00)*, volume 19, 3 of *Computer Graphics Forum*, pages 131–138, Cambridge, August 21–25 2000. Blackwell Publishers.
5. M. J. D. Powell and M. A. Sabin. Piecewise quadratic approximations on triangles. *ACM Transactions on Mathematical Software*, 3:316–325, 1977.
6. X. Shi, S. Wang, W. Wang, and R. H. Wang. The C^1 quadratic spline space on triangulations. *Report 86004, Department of Mathematics, Jilin University, Changchun*, 1986.
7. E. Vanraes, J. Maes, and A. Bultheel. Powell–Sabin spline wavelets. TW Report 362, Department of Computer Science, Katholieke Universiteit Leuven, Belgium, June 2003.
8. E. Vanraes, J. Windmolders, A. Bultheel, and P. Dierckx. Dyadic and $\sqrt{3}$–subdivision for Uniform Powell–Sabin splines. In *Information Visualisation Proceedings*. IEEE Computer Society, 2002.
9. J. Windmolders and P. Dierckx. Subdivision of Uniform Powell–Sabin splines. *CAGD*, 16(4):301–315, 1999.
10. J. Windmolders, E. Vanraes, P. Dierckx, and A. Bultheel. Uniform Powell–Sabin spline wavelets. TW Report 335, Department of Computer Science, Katholieke Universiteit Leuven, Belgium, February 2002.